

Collider Phenomenology of the Higgsless Models

Andreas Birkedal¹, Konstantin Matchev¹, and Maxim Perelstein²

¹ *Physics Department, University of Florida, Gainesville, FL 32611*

² *Institute for High-Energy Phenomenology, Cornell University, Ithaca, NY 14853*

(April 5, 2005)

We identify and study the signatures of the recently proposed Higgsless models at the Large Hadron Collider (LHC). We concentrate on tests of the mechanism of partial unitarity restoration in the longitudinal vector boson scattering, which is crucial to the phenomenological success of any Higgsless model and does not depend on the model-building details. We investigate the discovery reach for charged massive vector boson resonances and show that all of the preferred parameter space will be probed with 100 fb⁻¹ of LHC data. Unitarity restoration requires that the masses and couplings of the resonances obey certain sum rules. We discuss the prospects for their experimental verification at the LHC.

Introduction — Numerous experiments in high-energy physics confirm that the electromagnetic and weak interactions can be understood in terms of a non-abelian gauge theory with spontaneously broken "electroweak" $SU(2)_L \times U(1)_Y$ symmetry. The mechanism of the electroweak symmetry breaking (EWSB) is at present unknown. The suggested mechanisms may be roughly divided into those involving only weakly coupled physics (of which the Standard Model, perhaps supplemented by supersymmetry, is the best-known example), and those that rely on strong dynamics to break the symmetry, as in technicolor models [1]. A simple estimate for the scale of strong dynamics in theories of the second type, based on the unitarity violation in the scattering of longitudinal massive gauge bosons, gives

$$\Lambda \sim 4\pi M_W/g \sim 1.8 \text{ TeV}, \quad (1)$$

where g is the $SU(2)_L$ gauge coupling. The strongly coupled physics at this scale is generically ruled out by precision electroweak constraints (PEC), seemingly disfavoring the idea of the EWSB by strong dynamics [2]. Recently, however, this idea was implemented in a novel way in the "Higgsless" models [3–6]. In these models, new weakly coupled particles appear at the TeV scale and postpone unitarity violation [7], raising the strong coupling scale well above the naive estimate (1). As a result, the models have a better chance of achieving consistency with the PEC. In fact, while the original Higgsless models did not allow to raise Λ significantly without running into conflict with PEC [8–10], it was recently shown that Λ can be raised by at least a factor of 10 with appropriate modifications of the fermion sector [11].

In this letter, we would like to identify and study the collider signatures of the Higgsless models at the Large Hadron Collider (LHC). In realistic models, the strong coupling scale Λ is too high for the LHC to directly observe the strongly coupled physics responsible for the EWSB. On the other hand, the additional weakly coupled states required to raise Λ will be observable. A number of Higgsless models have been proposed in the literature, differing in the number of spatial dimensions (five in the original models, four in the "deconstructed" versions [12]), the embedding of the Standard Model (SM)

fermions, and so on. The spectrum of the TeV scale states and their interactions with the SM particles are highly model-dependent. The *mechanism* by which Λ is raised, however, is the same in all models: new massive vector bosons (MVBs), with the same quantum numbers as the familiar W , Z and γ , appear at the TeV scale. The couplings between the MVBs and the SM W/Z gauge bosons obey (at least approximately) *unitarity sum rules*, which enforce the cancellation of the fast-growing terms in the longitudinal gauge boson scattering amplitudes, postponing the unitarity violation. We will concentrate on the experimental signatures that test this mechanism, and are therefore independent of the details of specific Higgsless models.

Unitarity Sum Rules — Consider the elastic scattering process $W_L^\pm Z_L \rightarrow W_L^\pm Z_L$. In the absence of the Higgs boson, this process receives contributions from the three Feynman diagrams shown in Figs. 1 (a) – (c). Evaluating these diagrams yields the amplitude

$$\begin{aligned} \mathcal{M}^{\pm 0 \pm 0} &= (g_{\text{wwzz}} - g_{\text{wwz}}^2) \cdot \left[(c^2 - 6c - 3)E^4 \right. \\ &+ (c^2 - 3c - 2)M_Z^2 E^2 - (c^2 - 9c - 4)M_W^2 E^2 \left. \right] \\ &+ g_{\text{wwz}}^2 \frac{M_Z^4(1-c)}{2M_W^2} E^2 + \mathcal{O}(E^0), \end{aligned} \quad (2)$$

where $E \gg M_{W,Z}$ is the energy of the incoming W boson in the center of mass frame, c is the cosine of the scattering angle (the angle between the incoming and outgoing W bosons), the overall factor of $iM_W^{-2}M_Z^{-2}$ has been omitted, and the notation used for the coupling strengths is self-explanatory. In the Higgsless theories, this process receives an additional contribution from the diagrams in Figs. 1 (d) and (e), where V_i^\pm denotes the charged MVB of mass M_i^\pm (the Lorentz structure of the $V^\pm W^\mp Z$ coupling is identical to the familiar SM $W^\pm W^\mp Z$ vertex). The index i corresponds to the KK level of the state in the case of a 5D theory, or labels the mass eigenstates in the case of a 4D deconstructed theory. At high energies ($E \gg M_i^\pm$) the contribution of V_i^\pm is given by

$$\Delta \mathcal{M}_V^{\pm 0 \pm 0} = -(g_{\text{wzv}}^{(i)})^2 \left[(c^2 - 6c - 3)E^4 \right]$$

$$\begin{aligned}
& + (c^2 - 2c - 3)M_Z^2 E^2 - (c^2 - 10c - 3)M_W^2 E^2 \\
& + (1 - c) \frac{3(M_i^\pm)^4 - (M_W^2 - M_Z^2)^2}{2(M_i^\pm)^2} E^2 \Big] + \mathcal{O}(E^0). \quad (3)
\end{aligned}$$

The notation for the three-point coupling strength is again self-explanatory, and the overall factor of $iM_W^{-2}M_Z^{-2}$ has been dropped. Note that there is no diagram involving neutral MVBs, V_i^0 — the quantum numbers forbid three-point and four-point couplings involving exclusively neutral states. Remarkably, the E^4 and E^2 terms in Eq. (2) can be exactly cancelled by the contribution of the MVBs, provided that the following sum rules are satisfied:

$$\begin{aligned}
g_{\text{wwzz}} &= g_{\text{wwz}}^2 + \sum_i (g_{\text{wzv}}^{(i)})^2, \\
2(g_{\text{wwzz}} - g_{\text{wwz}}^2)(M_W^2 + M_Z^2) + g_{\text{wwz}}^2 \frac{M_Z^4}{M_W^2} \\
&= \sum_i (g_{\text{wzv}}^{(i)})^2 \left[3(M_i^\pm)^2 - \frac{(M_Z^2 - M_W^2)^2}{(M_i^\pm)^2} \right]. \quad (4)
\end{aligned}$$

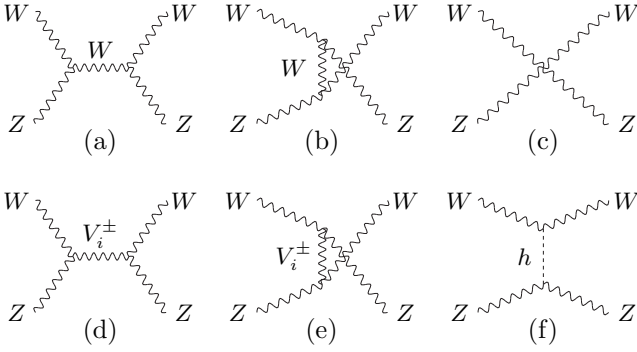


FIG. 1. Diagrams contributing to the $W^\pm Z \rightarrow W^\pm Z$ scattering process: (a), (b) and (c) appear both in the SM and in Higgsless models, (d) and (e) only appear in Higgsless models, while (f) only appears in the SM.

In 5D theories, these equations are satisfied exactly if all the KK states, $i = 1 \dots \infty$, are taken into account. This is not an accident, but a consequence of the gauge symmetry and locality of the underlying theory. While this is not sufficient to ensure unitarity at all energies (the increasing number of inelastic channels ultimately results in unitarity violation), the strong coupling scale can be significantly higher than the naive estimate (1). For example, in the warped-space Higgsless models [4,11] unitarity is violated at the scale [13]

$$\Lambda_{\text{NDA}} \sim \frac{3\pi^4}{g^2} \frac{M_W^2}{M_1^\pm}, \quad (5)$$

which is typically of order 5–10 TeV. In 4D models, the number of the MVBs is finite and the second of the sum

rules (4) is only satisfied approximately; however, a numerical study of sample models indicates that the violation of the sum rule has to be very small (at the level of 1%) to achieve an adequate improvement in Λ [14].

Considering the $W_L^+ W_L^- \rightarrow W_L^+ W_L^-$ scattering process yields the sum rules constraining the couplings of the neutral MVBs V_i^0 [3]:

$$\begin{aligned}
g_{\text{wwww}} &= g_{\text{wwz}}^2 + g_{\text{ww}\gamma}^2 + \sum_i (g_{\text{wwv}}^{(i)})^2, \\
4g_{\text{wwww}} M_W^2 &= 3 \left[g_{\text{wwz}}^2 M_Z^2 + \sum_i (g_{\text{wwv}}^{(i)})^2 (M_i^0)^2 \right], \quad (6)
\end{aligned}$$

where M_i^0 is the mass of the V_i^0 boson. Considering other channels such as $W_L^+ W_L^- \rightarrow ZZ$ and $ZZ \rightarrow ZZ$ does not yield any new sum rules. The presence of multiple MVBs, whose couplings obey Eqs. (4), (6), is a generic prediction of the Higgsless models.

Collider Phenomenology— Our study of the collider phenomenology in the Higgsless models will focus on the vector boson fusion processes. These processes are attractive for two reasons. Firstly, the production of the MVBs via vector boson fusion is relatively model-independent, since the couplings are constrained by the sum rules (4), (6). This is in sharp contrast with the Drell-Yan production mechanism [9], which dominates for the conventional W' and Z' bosons but is likely to be suppressed for the Higgsless MVBs due to their small couplings to fermions, which is needed to evade PEC [11]. Secondly, if enough couplings and masses can be measured, these processes can provide a *test* of the sum rules, probing the mechanism of partial unitarity restoration.

Eq. (5) indicates that the first MVB should appear below ~ 1 TeV, and thus be accessible at the LHC. For V_1^\pm , the sum rules (4) imply an inequality

$$g_{\text{wzv}}^{(1)} \lesssim \frac{g_{\text{wwz}} M_Z^2}{\sqrt{3} M_1^\pm M_W}. \quad (7)$$

This bound is quite stringent ($g_{\text{wzv}}^{(1)} \lesssim 0.04$ for $M_1^\pm = 700$ GeV). At the same time, convergence of the sum rules in (4) requires

$$g_{\text{wzv}}^{(k)} \propto k^{-1/2} (M_k^\pm)^{-1}. \quad (8)$$

The combination of heavier masses and lower couplings means that the heavier MVBs may well be unobservable, so that only the V_1 states can be studied. On the other hand, a numerical study of sample models indicates that the unitarity sum rules converge quite rapidly [14]. The "saturation limit", in which there is only a single set of MVBs whose couplings saturate the sum rules, is likely to provide a good approximation to the phenomenology of the realistic Higgsless models. In this limit, the partial width of the V_1^\pm is given by

$$\Gamma(V_1^\pm \rightarrow W^\pm Z) \approx \frac{\alpha (M_1^\pm)^3}{144 s_w^2 M_W^2}, \quad (9)$$

where $s_w \equiv \sin \theta_W$ is sine of the Weinberg angle. This formula is analogous, but not identical, to the well-known KSFR relation [15].

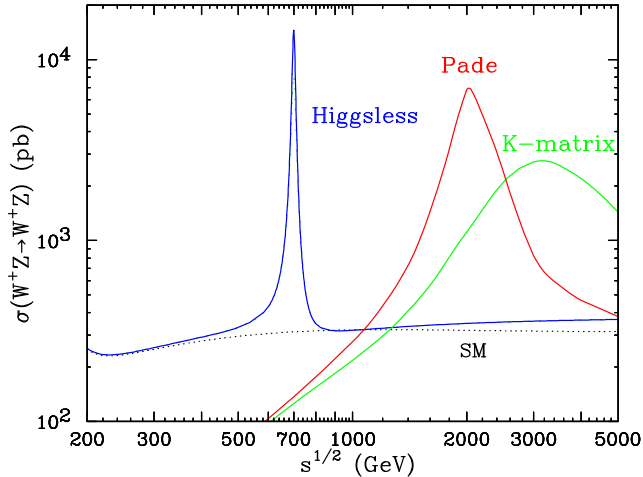


FIG. 2. WZ elastic scattering cross-sections in the SM (dotted), the Higgsless model (blue), and two "unitarization" models: Padé (red) and K-matrix (green).

A particularly interesting scattering channel is $WZ \rightarrow WZ$. In this channel, the Higgsless model predicts a series of resonances, see Fig. 1(d). In the Standard Model, on the other hand, this amplitude is unitarized by the t -channel Higgs exchange as in Fig. 1(f), and has no resonance. Conventional theories of EWSB by strong dynamics may contain a resonance in this channel, but it is likely to be heavy (~ 2 TeV for QCD-like theories) and broad due to strong coupling. An illustration is provided by Fig. 2, showing the parton-level cross section for this process in a Higgsless model in the saturation limit with a 700 GeV charged MVB V_1^\pm . We assume that the V_1^\pm has no significant couplings to fermions. With these assumptions the V_1^\pm width is about 15 GeV. For comparison, the figure shows the cross section in the SM with a 700 GeV Higgs, and in two phenomenological "unitarization models" which attempt to mimic the physics of the conventional technicolor-type theories: the Padé approximant and K-matrix schemes defined in Ref. [16] and available in the PYTHIA general purpose event generator. (The parameters used in Fig. 2 were obtained in [16] by "scaling up" the parameters of the pion chiral lagrangian; in the notation of [16], $M_R(\mu = 2 \text{ TeV}) = -9 \times 10^{-4}$, $N_R(\mu = 2 \text{ TeV}) = 1.8 \times 10^{-3}$.)

A striking feature of the charged MVB resonance is its small width: the resonance is almost a factor of 20 narrower than a SM Higgs of the same mass. This is primarily due to the vector nature of the MVB and the fact that it only has a single decay channel. At the same time, the coupling between the MVB and the SM gauge bosons is of a strength similar to the SM Higgs, as required for the unitarization of the $I = 0, J = 0$ channel in the Higgsless models.

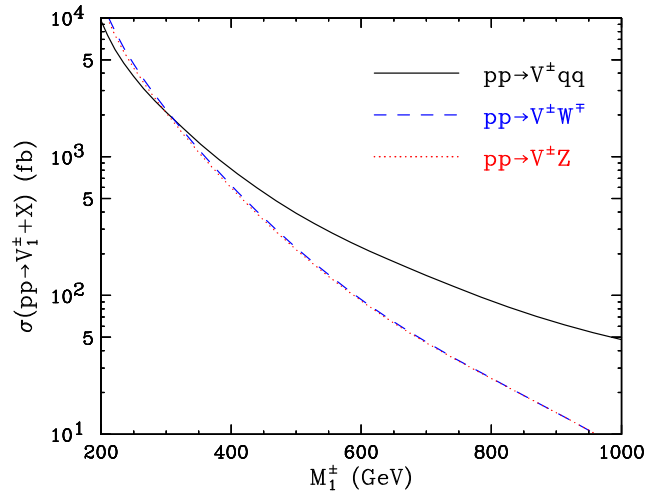


FIG. 3. Production cross-sections of V^\pm at the LHC.

At the LHC, the vector boson fusion processes will occur as a result of W/Z bremsstrahlung off quarks. The typical final state for such events includes two forward jets in addition to a pair of gauge bosons. The production cross section of V_1^\pm in association with two jets is shown by the solid line in Fig. 3. To estimate the prospects for the charged MVB search at the LHC, we require that both jets be observable (we assume jet rapidity coverage of $|\eta| \leq 4.5$), and impose the following lower cuts on the jet rapidity, energy, and transverse momentum: $|\eta| > 2$, $E > 300$ GeV, $p_T > 30$ GeV. These requirements enhance the contribution of the vector boson fusion diagrams relative to the irreducible background of the non-fusion $q\bar{q}' \rightarrow WZ$ SM process as well as $q\bar{q}' \rightarrow V_1^\pm$ Drell-Yan process. The "gold-plated" final state [17] for this search is $2j + 3\ell + \cancel{E}_T$, with the additional kinematic requirement that two of the leptons have to be consistent with a Z decay [18]. We assume lepton rapidity coverage of $|\eta| < 2.5$. The WZ invariant mass, m_{WZ} , can be reconstructed using the missing transverse energy measurement and requiring that the neutrino and the odd lepton form a W . The number of "gold-plated" events (including all lepton sign combinations) in a 300 fb^{-1} LHC data sample, as a function of m_{WZ} , is shown in Fig. 4. For comparison, this figure also shows the predictions of the four models discussed above, with the same assumptions as in Fig. 2. The Higgsless model can be easily identified by observing the MVB resonance: for the chosen parameters, the dataset contains 130 $V_1^\pm \rightarrow W^\pm Z \rightarrow 3\ell + \nu$ events. The irreducible non-fusion SM background is effectively suppressed by the cuts: the entire dataset shown in Fig. 4 contains only 6 such events. We therefore estimate the discovery reach for V_1^\pm resonance by requiring 10 signal events after cuts. The efficiency of the cuts for $500 \text{ GeV} \leq M_1^\pm \leq 3 \text{ TeV}$ is in the range 20 – 25%. We then find that with 10 fb^{-1} of data, corresponding to 1 year of running at low luminosity, the LHC will probe the Higgsless models up to $M_1^\pm \lesssim 550$ GeV, while covering

the whole preferred range up to $M_1^\pm = 1$ TeV requires 60 fb^{-1} . Note, however, that one should expect a certain amount of reducible background with fake and/or non-isolated leptons.

Once the V_1^\pm resonance is discovered, identifying it as part of a Higgsless model requires testing the sum rules (4) by measuring its mass M_1^\pm and coupling $g_{WZV}^{(1)}$. The coupling can be determined from the total V_1^\pm production cross section σ_{tot} . However, we are observing the V_1^\pm resonance in an exclusive channel, which only yields the product $\sigma_{\text{tot}} BR(V_1^\pm \rightarrow W^\pm Z)$. A measurement of the total resonance width $\Gamma(V_1^\pm \rightarrow \text{anything})$ would remove the dependence on the unknown branching fraction BR . However, the accuracy of this measurement is severely limited by the poor missing energy resolution. Nevertheless, a Higgsless origin of the resonance can be ruled out if the value of $g_{WZV}^{(1)}$, inferred with the assumption of $BR = 1$, violates the bound (7).

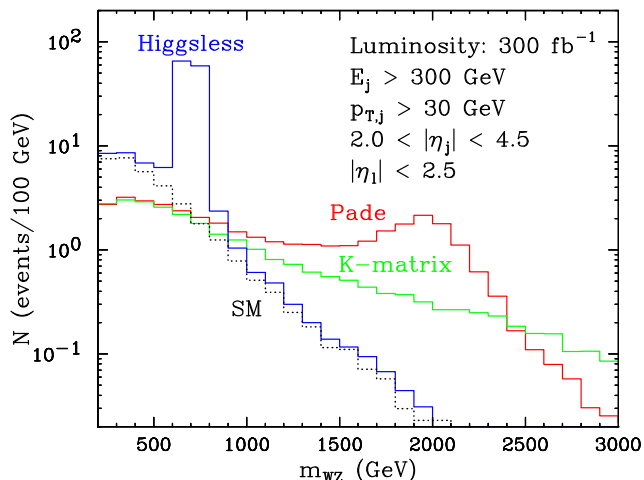


FIG. 4. The number of events per 100 GeV bin in the $2j + 3l + \nu$ channel at the LHC with an integrated luminosity of 300 fb^{-1} and cuts as indicated in the figure. The model assumptions and parameter choices are the same as in Fig. 2.

By transferring a Z or a W^\pm from the initial state to the final state in Figs. 1 (d) and (e), we obtain an alternative V_1^\pm production process, the associated production, which can be used for discovery as well as testing the sum rules (4). The total cross section for this process is shown in Fig. 3. The $W^\pm ZZ$ final state, with the requirement that all three gauge bosons decay leptonically, yields a very clean $5l + \cancel{E}_T$ signature. One can then reconstruct the two Z 's and the V_1^\pm resonance. The main advantage of this purely leptonic channel would be the superior measurement of the total width; however, the analysis is statistics limited and the discovery reach does not extend beyond 500 GeV, even for the high-luminosity LHC option.

Conclusions — It has long been known that the vector boson fusion processes will provide an important tool for testing the strongly coupled theories of EWSB at the

LHC. This is as true for the recently proposed Higgsless models as it is for traditional technicolor theories. As we discussed in this letter, the observation of a light and narrow resonance in the WZ channel would be a smoking gun for the Higgsless models. In addition, the Higgsless models provide a robust, definite prediction concerning the properties of the resonance, the sum rules (4), which can also be tested in this channel.

While we have concentrated on the WZ channel which provides the most striking signals, other vector boson fusion processes may also be useful. The neutral MVBs V_i^0 would appear as resonances in the W^+W^- channel; however, reconstructing these resonances requires hadronic W decays and suffers from severe backgrounds [19]. The ZZ channel exhibits no resonance, but could provide an independent test of the model. These channels will be explored in more detail in [14].

Acknowledgments — We would like to thank C. Csáki and G. Cacciapaglia for helpful discussions. MP is supported by NSF grant PHY-0355005. KM and AB are supported by a US DoE Outstanding Junior Investigator award under grant DE-FG02-97ER41029. MP would like to thank the theory group at the University of Florida for their hospitality during the completion of this work.

-
- [1] S. Dimopoulos and L. Susskind, Nucl. Phys. B **155**, 237 (1979); L. Susskind, Phys. Rev. D **20**, 2619 (1979); S. Weinberg, Phys. Rev. D **19**, 1277 (1979).
 - [2] M. E. Peskin and T. Takeuchi, Phys. Rev. Lett. **65**, 964 (1990); Phys. Rev. D **46**, 381 (1992).
 - [3] C. Csaki, C. Grojean, H. Murayama, L. Pilo and J. Terning, Phys. Rev. D **69**, 055006 (2004) [arXiv:hep-ph/0305237].
 - [4] C. Csaki, C. Grojean, L. Pilo and J. Terning, Phys. Rev. Lett. **92**, 101802 (2004) [arXiv:hep-ph/0308038].
 - [5] Y. Nomura, JHEP **0311**, 050 (2003) [arXiv:hep-ph/0309189].
 - [6] C. Csaki, C. Grojean, J. Hubisz, Y. Shirman and J. Terning, Phys. Rev. D **70**, 015012 (2004) [arXiv:hep-ph/0310355].
 - [7] R. Sekhar Chivukula, D. A. Dicus and H. J. He, Phys. Lett. B **525**, 175 (2002) [arXiv:hep-ph/0111016].
 - [8] R. Barbieri, A. Pomarol and R. Rattazzi, Phys. Lett. B **591**, 141 (2004) [arXiv:hep-ph/0310285]; G. Burdman and Y. Nomura, Phys. Rev. D **69**, 115013 (2004) [arXiv:hep-ph/0312247]; G. Cacciapaglia, C. Csaki, C. Grojean and J. Terning, Phys. Rev. D **70**, 075014 (2004) [arXiv:hep-ph/0401160].
 - [9] H. Davoudiasl, J. L. Hewett, B. Lillie and T. G. Rizzo, Phys. Rev. D **70**, 015006 (2004) [arXiv:hep-ph/0312193].
 - [10] H. Davoudiasl, J. L. Hewett, B. Lillie and T. G. Rizzo, JHEP **0405**, 015 (2004) [arXiv:hep-ph/0403300]; R. Barbieri, A. Pomarol, R. Rattazzi and A. Strumia, Nucl. Phys. B **703**, 127 (2004) [arXiv:hep-ph/0405040];

- J. L. Hewett, B. Lillie and T. G. Rizzo, JHEP **0410**, 014 (2004) [arXiv:hep-ph/0407059].
- [11] G. Cacciapaglia, C. Csaki, C. Grojean and J. Terning, Phys. Rev. D **71**, 035015 (2005) [arXiv:hep-ph/0409126]; R. Foadi, S. Gopalakrishna and C. Schmidt, Phys. Lett. B **606**, 157 (2005) [arXiv:hep-ph/0409266].
- [12] R. Foadi, S. Gopalakrishna and C. Schmidt, JHEP **0403**, 042 (2004) [arXiv:hep-ph/0312324]; R. Casalbuoni, S. De Curtis and D. Dominici, Phys. Rev. D **70**, 055010 (2004) [arXiv:hep-ph/0405188]; R. S. Chivukula *et al.*, Phys. Rev. D **70**, 075008 (2004) [arXiv:hep-ph/0406077]; H. Georgi, Phys. Rev. D **71**, 015016 (2005) [arXiv:hep-ph/0408067]; M. Perelstein, JHEP **0410**, 010 (2004) [arXiv:hep-ph/0408072].
- [13] M. Papucci, arXiv:hep-ph/0408058.
- [14] A. Birkedal, K. Matchev and M. Perelstein, to appear.
- [15] K. Kawarabayashi and M. Suzuki, Phys. Rev. Lett. **16**, 255 (1966); Riazuddin and Fayyazuddin, Phys. Rev. **147**, 1071 (1966).
- [16] A. Dobado, M. J. Herrero and J. Terron, Z. Phys. C **50** (1991) 205; see also A. Dobado and M. J. Herrero, Phys. Lett. B **228**, 495 (1989); Phys. Lett. B **233**, 505 (1989); A. Dobado, M. J. Herrero and J. Terron, Z. Phys. C **50** (1991) 465.
- [17] J. Bagger *et al.*, Phys. Rev. D **49**, 1246 (1994) [arXiv:hep-ph/9306256]; Phys. Rev. D **52**, 3878 (1995) [arXiv:hep-ph/9504426]. See also M. S. Chanowitz, arXiv:hep-ph/0412203 and references therein.
- [18] Other channels, such as $4j + 2l$, may also be useful, although the backgrounds are expected to be higher.
- [19] J. M. Butterworth, B. E. Cox and J. R. Forshaw, Phys. Rev. D **65**, 096014 (2002) [arXiv:hep-ph/0201098].